Magnetic particle imaging with a planar frequency mixing magnetic detection scanner

Hyobong Hong, Jaeho Lim, Chel-Jong Choi, Sung-Woong Shin, and Hans-Joachim Krause

Magnetic particle imaging with a planar frequency mixing magnetic detection scanner

Hyobong Hong,[1] Jaeho Lim,[1] Chel-Jong Choi,[2] Sung-Woong Shin,[1] and Hans-Joachim Krause[3,a)]

[1]*Spatial Information Technology Research Section, Electronics & Telecommunication Research Institute (ETRI), Daejeon 307-700, South Korea*
[2]*School of Semiconductor and Chemical Engineering, Semiconductor Physics Research Center (SPRC), Chonbuk National University, Jeonju 561-756, South Korea*
[3]*Peter Grünberg Institute (PGI-8), Forschungszentrum Jülich, 52425 Jülich, Germany*

We present the first experimental results of our planar-Frequency Mixing Magnetic Detection (p-FMMD) technique to obtain Magnetic Particles Imaging (MPI). The p-FMMD scanner consists of two magnetic measurement heads with intermediate space for the analysis of the sample. The magnetic signal originates from the nonlinear magnetization characteristics of superparamagnetic particles as in case of the usual MPI scanner. However, the detection principle is different. Standard MPI records the higher order harmonic response of particles at a field-free point or line. By contrast, FMMD records a sum-frequency component generated from both a high and a low frequency magnetic field incident on the magnetically nonlinear particles. As compared to conventional MPI scanner, there is no limit on the lateral dimensions of the sample; just the sample height is limited to 2 mm. In addition, the technique does not require a strong magnetic field or gradient because of the mixing of the two different frequencies. In this study, we acquired an 18 mm × 18 mm image of a string sample decorated with 100 nm diameter magnetic particles, using the p-FMMD technique. The results showed that it is feasible to use this novel MPI scanner for biological analysis and medical diagnostic purposes. © *2014 AIP Publishing LLC*. [http://dx.doi.org/10.1063/1.4861916]

I. INTRODUCTION

Magnetic particles have been used for the manipulation of cells and biomolecules or for selectively labeling materials for detection.[1,2] Recently, their application range has been extended to medical imaging, where they serve as contrast agents or tracers for MRI, SQUID, or similar techniques.[1,3] This is because magnetic nanoparticles usually exhibit superparamagnetic properties, whereas the human body is dia- or para-magnetic.[4] Thus, many efforts have been taken to use the particles to obtain medical images because of the relatively high sensitivity and spatial resolution. A Magnetic Particles Imaging (MPI) scanner comprises two essential techniques. The first one is obtaining non-linear signals from the magnetic particles. In previous research, higher-order harmonic signals from the magnetization response were recorded, corresponding to the nonlinear properties of magnetic nanoparticles exposed to a magnetic field. The second is the reconstruction of the image based on the determination of the spatial distribution of the magnetic particles. In order to get spatial distribution information, two methods are usually employed, the mechanical movement of the sensor with respect to the sample, or the movement of field-free point by means of electromagnets.[1,2]

In 2005, Gleich and Weizenecker introduced the MPI scanner which consists of two pairs of transmit coils and two pairs of smaller receive coils.[5] In the study, two pairs of transmit coils generated a field-free point (FFP), where magnetic particles are not saturated magnetically. Therefore, they produce a nonlinear magnetic response signal. With the movement of FFP and employment of the receiver coils, they acquired MPI images with a spatial resolution of 1.0 mm. Goodwill *et al.* obtained 2D or 3D MPI with the same principle, but with a different image re-construction.[6,7] A single-sided scanner for magnetic particle imaging was presented by Gräfe *et al.*[8] It relies on the same principle, but avoids the problem of fitting the specimen into the scanner.

Up to date, two image re-construction methods have been suggested, harmonic-space MPI and X-space MPI. Harmonic space MPI relies on a system matrix to pre-characterize the signal response of the magnetic nanoparticles.[2] Goodwill *et al.* introduced a new image re-construction method called X-space MPI.[9] They showed that X-space MPI has several advantages over harmonic space MPI, such as offering experimentally proven linearity and shift invariance. In addition, the convolution of the MPI signals leads to improved resolution over the native resolution, which is determined by the physics of the nanoparticles and the field gradient, showing the improvement of both robustness and speed.

Recently, a new magnetic detection method was developed which is based on frequency mixing at the non-linear magnetization curve of superparamagnetic particles.[10] When super-paramagnets are exposed to magnetic fields at two distinct frequencies (f_1 and f_2), sum frequencies representing a linear combination $mf_1 + nf_2$ (with integer numbers m, n) are

a)Author to whom correspondence should be addressed. Electronic mail: h.-j.krause@fz-juelich.de
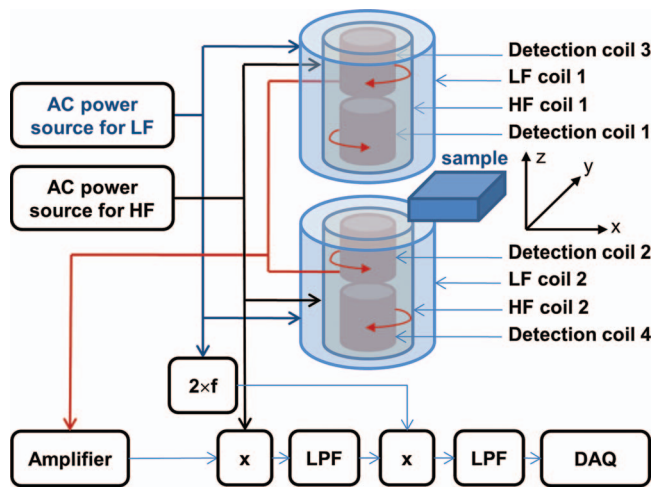
FIG. 1. Schematic drawing of the p-FMMD set-up. Two measurement heads are electronically connected to each other. The sample is placed in the space between the heads. Detection coils 1 and 2 measure the sample signal; counter-wound detection coils 3 and 4 serve as reference to cancel out the direct field from the HF and LF coils. $2 \times f$ – frequency doubler, x – mixer, LPF – low pass filter, DAQ – data acquisition.

of 0.4 mT at $f_1 = 76.55$ kHz, the low frequency coil produces 5 mT at $f_2 = 61$ Hz. A XYZ motorized stage was purchased from Sciencetown (Incheon, Korea). Magnetic beads with a diameter of 100 nm (FluidMAG-Amine) were purchased from Chemicell (Berlin, Germany). The solution was washed three times and diluted to one to ten times with distilled water. Two types of samples were prepared, a paper pellet (Fig. 3) and a string (Fig. 4). The samples were soaked in magnetic bead solution for 30 s and dried in air. For the measurement, the sample was fixed on top of the sample holder. The speed of XYZ stage was adjusted to values between 1.0 and 7.0 mm/s. The XYZ stage moved the planar-FMMD measurement head from the lower right corner to the upper left of a square region with subsequent horizontal lines, covering a 18.0×18.0 mm^2 region. The scanner moves along the x-axis in 18 mm long traces and steps in y-direction by 0.96 mm. At a stage speed of 1.0 mm/s, this amounts to a scanning time of 10 min. With 7.0 mm/s, the image is acquired in 1.5 min. The image was constructed by converting the raw data to matrix form and obtaining a contour image using Origin 8.5.

generated. It was shown that the appearance of these components is highly specific to the nonlinearity of the magnetization curve of the particles.[11] A new type of MPI scanner employing this technique was prepared (see Fig. 1) and applied to obtain MPI images of planar samples. The results showed the applicability of the new MPI scanner to a broad range of potential applications. Previous research showed that it can be applied to areas such as cardiovascular, cancer imaging, and the other diagnostic purposes.[12]

II. METHODS

The planar-Frequency Mixing Magnetic Detection (p-FMMD) scanner consists of a magnetic measurement head, controllers, and a XYZ-motorized stage. The p-FMMD uses two sets of excitation and detection coils attached above and below the sample, with 2 mm space in between them. A schematic diagram of the p-FMMD is shown in Figure 1. Each set of coils consists of a low frequency driver coil, a high frequency excitation coil, and a differential detection coil comprising two oppositely wound pickup coils in axial gradiometer configuration. The detailed parameters of the coils are listed in Table I. The high frequency coil generates a field

III. RESULTS AND DISCUSSION

A schematic drawing of the measurement head is depicted in Fig. 1. Details of the FMMD principle and of the readout electronics have been published,[10,11] so only a brief explanation is given here. The measurement technique is based on the nonlinearity of the magnetization curve of the superparamagnetic particles with the application of two magnetic excitation fields of different frequency on the sample, a low frequency (f_2) component to drive the particles into magnetic saturation and a high frequency (f_1) probe field. The frequency mixing components are detected by the differentially wound pickup coil. The differences in the magnetic field between the measuring coil and the blank coil due to the presence of super-paramagnetic materials are then measurable and quantifiable. In the readout electronics, the intermodulation product at sum frequency $f_1 + 2f_2$ is demodulated. It was shown that this technique allows fast processing and a very large dynamic detection range. Principally, the conventional hardware of MPI consists of the magnets generating a main field gradient, also known as a selection field, analog signal chain (the transmit and receive sub-systems), and raster pulse sequence. Thus, our 2D scanning method is a different technique as compared to conventional MPI based on generating

TABLE I. Parameters of the coils of the measurement head.

Coil	Coil dimensions			Windings		Coil below sample		Coil above sample	
	R_1 (mm)[a]	W (mm)[b]	H (mm)[c]	No. of windgs	Wire-ø (mm)	R (Ω)[d]	L (mH)[e]	R (Ω)[d]	L (mH)[e]
Measurement	1	4	1.7	2×600	0.08	47.67	0.95	47.66	0.95
Excitation	3.8	8.5	1	476	0.10	29.90	1.56	29.70	1.453
Driver	5	8.5	5	2000	0.12	190.75	36.9	141.28	37.9

[a]R_1 is the inner radius of the coil. The average radius is $R_1 + H/2$, the outer radius is $R_1 + H$.
[b]W is the width of the coil, i.e., the cross section of the windings.
[c]H is the height of the coil windings.
[d]R denotes the Ohmic resistance at DC. In case of the measurement coils, it is the series resistance of both coils.
[e]L denotes the inductance, measured with an inductance meter at 1 kHz.
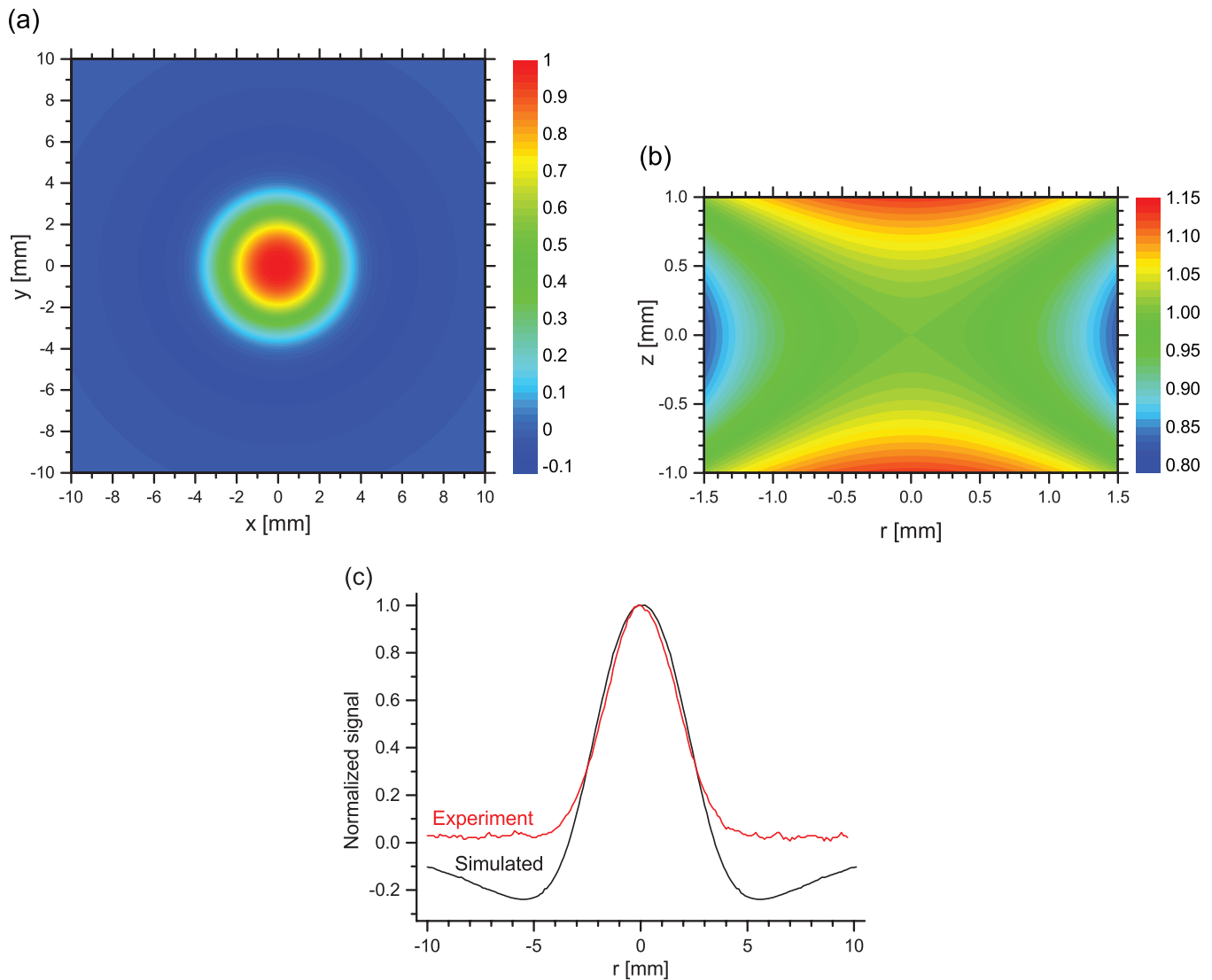
(a)

(b)

(c)

FIG. 2. Graphical representation of the calculated sensitivity distribution of the measurement head (a) as a function of the planar coordinates x and y for $z = 0$, (b) as a function of the axial coordinate z and the radial coordinate r. The sensitivity is given relatively to the center between the upper and lower detection coil at $x = 0$, $y = 0$, and $r = 0$. (c) Comparison of measured and simulated sensitivity.

a Field Free Point (FFP) or Field Free Line (FFL), although the detection based on the non-linear signal from superparamagnets is similar.[2,13] Although the conventional MPI has advantages over the new MPI scanner suggested herein, such as the simultaneous 3D analysis without mechanical movement of sample or system,[7] the new MPI scanner does not need a relatively strong field and has no limitations for the XY axis. We believe that both the conventional MPI scanner and the p-FMMD scanner have their specific advantages. The advantage of the p-FMMD scanner is its simplicity and its small dimensions. However, it is not applicable to thick samples. Figure 2(a) shows the sensitivity distribution of the inner double-differential detection coil as a function of the planar coordinates x and y. It is determined by calculating the superposition of the magnetic field generated by all 4 detection coils. The calculation is performed by approximating the coils as long coils of negligible height, using the textbook elliptic integral formula. Thus, Fig. 2(a) represents the sensitivity map in the scanning plane, the so-called point spread function

(PSF). Figure 2(b) shows the sensitivity as a function of the axial coordinate z and the radial coordinate r, thus giving a vertical mapping of the sensitivity in the slit of the measurement head. The origin $x = 0$ and $y = 0$ is lying exactly in the center of the detection coil. The physical detection limit of the coil (parameters: inner coil radius $R_1 = 1$ mm, coil width $W = 4$ mm, coil height $H = 1.7$ mm, axis position $Z = 3.6$ mm, filling factor (i.e., the copper fraction in the windings cross section) $K_F = 0.5$, frequency of the HF excitation $f_1 = 76.55$ kHz) with respect to magnetic moments at the center was calculated to be $m_0/\sqrt{f} = 1.8 \times 10^{-14}$ Am^2/$\sqrt{\text{Hz}}$. For 10 s measurement time, this amounts to a resolution of $m_0 = 2.3 \times 10^{-14}$ Am^2. As depicted, the detection coil has an outer diameter of 5.4 mm. The spacing between the centers of the upper and lower detection coil is 2 mm. So the radius of the detection part is about 3 mm. More detailed parameters are summarized in Table I. Figure 2(c) shows the experimental scan over the string-type line sample and, for comparison, a calculated sensitivity trace. The latter one was calculated
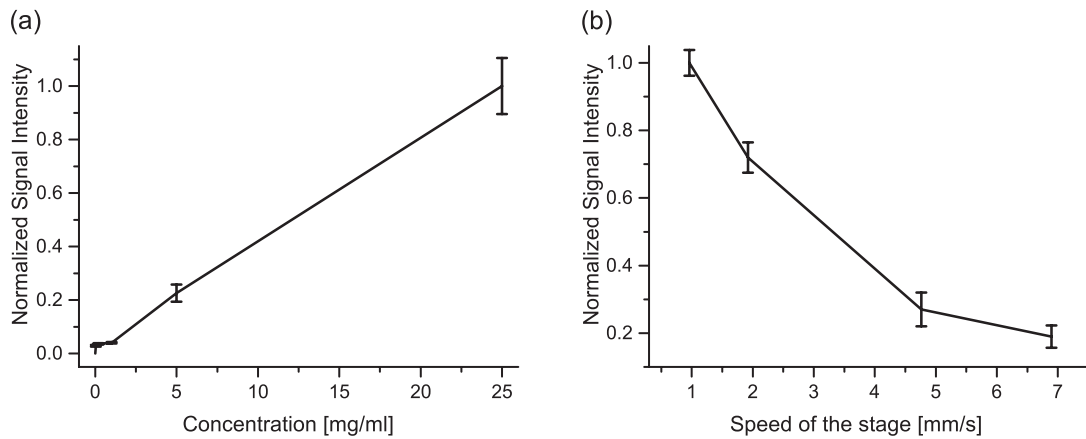
FIG. 3. Normalized calibration curve of (a) the p-FMMD measurement using different concentrations of magnetic beads. As samples, paper pellets with 2.0 mm diameter were prepared using a Biopsy Punch from Integra (New Jersey), soaked in magnetic particle solution of different concentrations. The measurement head passed the paper pellets with different concentrations of MP. The speed of the stage was adjusted to 1.0 mm/s. (b) Decrease of the signal intensity as function of the speed of the XY stage for the 5.0 mg/ml paper pellet sample.

by numerically integrating the point spread function depicted in Fig. 2(a) over a 2 mm wide ideal line. The agreement is good, except that the negative shoulders in the calculated signal, which are due to the reference coils, are not observed experimentally. This is attributed to the fact that the coil in the simulation is approximated with negligible height of windings.

Figure 3(a) shows the relationship between the movement speeds of XYZ stage and signal intensity showing that higher signals can be obtained at the lower speed. Figure 3(b) shows the signal intensity as a function of the concentration of magnetic beads solution. Speed is adjusted to 1.0 cm/min and the concentration is changed from 0.04 to 25.0 mg/ml. The results showed a strong correlation between the concentration of magnetic beads and signals from the detector. The R^2 value of the linear approximation was evaluated as 0.98. By the linear fit, an offset of -2.37 mV was determined for zero particle concentration for the results of Fig. 3.

The results indicated the spatial resolution and detection limit of p-FMMD is dependent on the speed of XY stage (or sample) and concentration of the magnetic particles. This is due to the low pass filter at the output of the two-stage lock-in detection of the readout electronics. Previous research also showed that spatial resolution is dependent on a few parameters such as speed of gradient strength, the particle diameter, volume of the magnetic core, and mechanical speed of the stage.[14] Figure 4 shows a photograph of the object and the reconstructed image. Although it is very clear to show the feasibility of p-FMMD as MPI scanner, the low MPI are broader and shorter than the real object. For the broader image, it is thought to be involved in two parameters. The first one is the sensitivity profile of the measurement head. As shown in Fig. 2(a), the measurement of a magnetic particle distribution is broadened by this distribution even to ± 2.0 mm from the center of the measurement heads. The second is the movement of y axis. The measurement head moves 0.96 mm along y-axis every end of x-axis movement. Although MPI image is interpolated by the software, there can be data omitted because of the y-axis movement resulting in the shortening the length of whole object which is crossing y-axis. Thus, the optimization of speed of XY stage and degree of y axis movement is assumed as the crucial point of this technique instead of the focusing of FFP or FFL which is essential for conventional MPI.
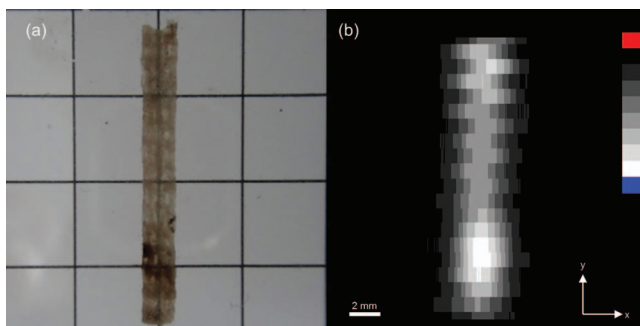

FIG. 4. (a) Photograph of the string type sample (on a 5 mm grid). The sample of dimension 2.0 mm × 18.0 mm was prepared using Cleanroom Wiper (CF-909, Seoul Semitech Co, LTD, Seoul, Korea). (b) Reconstructed MPI image. The sample is continuously scanned in x direction and consecutively stepped in y direction by 0.96 mm.

IV. CONCLUSION

MPI is a relatively new technique that has a variety of potential applications in many scientific and industrial fields. The study also showed that its spatial resolution is comparable with the other medical imaging. In this study, we introduced relatively new technique called p-FMMD to get MPI. Comparing with the other MPI scanner, it does not mainly dependent on the generation of FFP or FFL requiring the relatively strong magnetic field or generation of gradient field. Based on our researches, it is believed that p-FMMD technique will be the other feasible method in the field of MPI and will find many roles in the analysis of biological tissue sections for diagnostics and even for the invasive study of many diseases.

ACKNOWLEDGMENTS

[1]J. Borgert, J. D. Schmidt, I. Schmale, J. Rahmer, C. Bontus, B. Gleich, B. David, R. Eckart, O. Woywode, J. Weizenecker, J. Schnorr, M. Taupitz, J. Haegele, F. M. Vogt, and J. Barkhausen, "Fundamentals and applications of magnetic particle imaging," J Cardiovasc. Comput. Tomogr. **6**(3), 149–153 (2012).

[2]T. M. Buzug, G. Bringout, M. Erbe, K. Gräfe, M. Graeser, M. Gruttner, A. Halkola, T. F. Sattel, W. Tenner, H. Wojtczyk, J. Haegele, F. M. Vogt, J. Barkhausen, and K. Lüdtke-Buzug, "Magnetic particle imaging: Introduction to imaging and hardware realization," Z. Med. Phys. **22**(4), 323–334 (2012).

[3]E. U. Saritas, P. W. Goodwill, L. R. Croft, J. J. Konkle, K. Lu, B. Zheng, and S. M. Conolly, "Magnetic Particle Imaging (MPI) for NMR and MRI researchers," J. Magn. Reson. **229**(4), 116–126 (2013).

[4]P. W. Goodwill, E. U. Saritas, L. R. Croft, T. N. Kim, K. M. Krishnan, D. V. Schaffer, and S. M. Conolly, "X-space MPI: Magnetic nanoparticles for safe medical imaging," Adv. Mater. **24**(28), 3870–3877 (2012).

[5]B. Gleich and J. Weizenecker, "Tomographic imaging using the nonlinear response of magnetic particles," Nature (London) **435**(7046), 1214–1217 (2005).

[6]J. Rahmer, J. Weizenecker, B. Gleich, and J. Borgert, "Analysis of a 3-D system function measured for magnetic particle imaging," IEEE Trans. Med. Imaging **31**(6), 1289–1299 (2012).

[7]P. W. Goodwill and S. M. Conolly, "Multidimensional x-space magnetic particle imaging," IEEE Trans. Med. Imaging **30**(9), 1581–1590 (2011).

[8]K. Gräfe, T. F. Sattel, K. Lüdtke-Buzug, D. Finas, J. Borgert, and T. M. Buzug, "An application scenario for single-sided magnetic particle imaging," Biomed. Tech. **57**, Suppl. 1 (2012).

[9]P. W. Goodwill, J. J. Konkle, B. Zheng, E. U. Saritas, and S. M. Conolly, "Projection x-space magnetic particle imaging," IEEE Trans. Med. Imaging **31**(5), 1076–1085 (2012).

[10]H.-J. Krause, N. Wolters, Y. Zhang, A. Offenhäusser, P. Miethe, M. H. F. Meyer, M. Hartmann, and M. Keusgen, "Magnetic particle detection by frequency mixing for immunoassay applications," J. Magn. Magn. Mater. **311**(1), 436–444 (2007).

[11]M. H. F. Meyer, H.-J. Krause, M. Hartmann, P. Miethe, J. Oster, and M. Keusgen, "Francisella tularensis detection using magnetic labels and a magnetic biosensor based on frequency mixing," J. Magn. Magn. Mater. **311**(1), 259–263 (2007).

[12]D. Finas, K. Baumann, L. Sydow, K. Heinrich, K. Gräfe, T. Buzug, and K. Lüdtke-Buzug, "Detection and distribution of superparamagnetic nanoparticles in lymphatic tissue in a breast cancer model for magnetic particle imaging," Biomed Tech. **57**, Suppl. 1 (2012); J. Haegele, S. Biederer, H. Wojtczyk, M. Graser, T. Knopp, T. M. Buzug, J. Barkhausen, and F. M. Vogt, "Toward cardiovascular interventions guided by magnetic particle imaging: First instrument characterization," Magn. Reson. Med. **69**(6), 1761–1767 (2013); J. Haegele, J. Rahmer, B. Gleich, J. Borgert, H. Wojtczyk, N. Panagiotopoulos, T. M. Buzug, J. Barkhausen, and F. M. Vogt, "Magnetic particle imaging: Visualization of instruments for cardiovascular intervention," Radiology **265**(3), 933–938 (2012).

[13]J. Lampe, C. Bassoy, J. Rahmer, J. Weizenecker, H. Voss, B. Gleich, and J. Borgert, "Fast reconstruction in magnetic particle imaging," Phys. Med. Biol. **57**(4), 1113–1134 (2012).

[14]P. W. Goodwill, K. Lu, B. Zheng, and S. M. Conolly, "An x-space magnetic particle imaging scanner," Rev. Sci. Instrum. **83**(3), 033708 (2012).